

CREATING A SATELLITE-BASED RECORD OF TROPOSPHERIC OZONE

Hilke Oetjen¹, Vivienne H. Payne², Susan S. Kulawik^{2,3}, Annmarie Eldering^{1,2}, John Worden²,
David P. Edwards⁴, Gene L. Francis⁴, Helen M. Worden⁴

1. UCLA/JPL Joint Institute for Regional Earth System Science and Engineering, 607 Charles E. Young Dr. East., Los Angeles, CA 90095, United States
2. Jet Propulsion Laboratory, California Institute of Technology, 4800 Oak Grove Dr., La Canada Flintridge, CA 91011, United States
3. BAER Institute, 560 Third St. West, Sonoma, CA 95476, United States
4. National Center for Atmospheric Research, 3450 Mitchell Ln., Boulder, CO 80301, United States

Abstract

The TES retrieval algorithm has been applied to IASI radiances. We compare the retrieved ozone profiles with ozone sonde profiles for mid-latitudes for the year 2008. We find a positive bias in the IASI ozone profiles in the UTLS region of up to 22 %. The spatial coverage of the IASI instrument allows sampling of effectively the same air mass with several IASI scenes simultaneously. Comparisons of the root-mean-square of an ensemble of IASI profiles to theoretical errors indicate that the measurement noise and the interference of temperature and water vapour on the retrieval together mostly explain the empirically derived random errors. The total degrees of freedom for signal of the retrieval for ozone are 3.1 ± 0.2 and the tropospheric degrees of freedom are 1.0 ± 0.2 for the described cases. IASI ozone profiles agree within the error bars with coincident ozone profiles derived from a TES stare sequence for the ozone sonde station at Bratt's Lake (50.2°N , 104.7°W).

INTRODUCTION

Ozone acts as a toxic pollutant in the lower troposphere, a greenhouse gas in the upper troposphere and as a protective shield against harmful ultra-violet radiation in the stratosphere. Satellite-borne instruments provide the means for global and continuous monitoring of this important trace gas. High spectral resolution infrared radiance measurements, such as those from the Tropospheric Emission Spectrometer (TES) on the NASA Aura satellite (launched in 2004), and the Infrared Atmospheric Sounding Instruments (IASI), on the MetOp-A and MetOp-B satellites (launched in 2006 and 2012 respectively) can provide vertical information on tropospheric ozone. Together, these instruments now provide a record spanning more than eight years. As part of efforts to assess consistency between the TES and IASI data records, a retrieval for ozone from IASI radiances, building on the data processor for TES, is under development as a collaboration between NASA JPL and NCAR. Using a priori information consistent with TES retrievals, the optimal estimation approach is applied to IASI radiances in order to obtain vertical distributions of ozone. This paper shows comparisons of these retrievals with coincident ozone sonde profiles. The emphasis of this study is on the characterisation of the retrieval uncertainties and sensitivity.

IASI OZONE RETRIEVALS

The IASI instrument is a Fourier transform spectrometer measuring infrared radiances between 645 and 2760 cm^{-1} with a spectral resolution of 0.5 cm^{-1} (apodised). IASI is a nadir-viewing instrument and scans across the track within $\pm 48.3^{\circ}$ in a step and stare mode. There are 120 measurements per scan line and the surface footprint is circular with 12 km diameter at nadir. Global coverage is achieved twice daily. IASI was designed by the Centre National d'Etudes Spatiales (CNES) and launched

October 2006 onboard the MetOp-A satellite. More details of the instrument can be found in Clerbaux et al (2009).

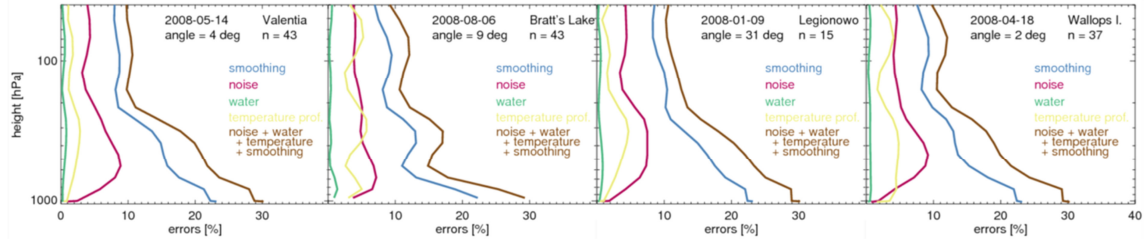


Figure 1: Theoretical errors for selected locations.

We apply an optimal estimation approach (Rodgers, 2000) following the TES algorithm to IASI L1c radiances to simultaneously retrieve ozone and water vapour profiles in the spectral windows 990–1031 cm^{-1} , 1040–1049 cm^{-1} , and 1069–1072 cm^{-1} . The optimal estimation approach minimises the cost function:

$$\mathbf{C} = \|\mathbf{y} - \mathbf{L}(\mathbf{x})\|_{\text{data noise}}^2 + \|\mathbf{z}_a \text{ priori} - \mathbf{z}\|_{\mathbf{S}_a}^2 \quad (1)$$

in a non-linear Levenberg-Marquardt iterative scheme (Bowman et al., 2006). \mathbf{y} is the measured radiance, a discrete vector, related to the true state \mathbf{L}^{true} by an additive noise model $\boldsymbol{\varepsilon}$:

$$\mathbf{y} = \mathbf{L}^{\text{true}} + \boldsymbol{\varepsilon} \quad (2)$$

\mathbf{L} can also be interpreted as an operator describing the radiative transfer dependent on the atmospheric state. Hence $\mathbf{L}(\mathbf{x})$ is the forward model of a specific state vector \mathbf{x} . The second term of (1) describes the difference between the a priori profile \mathbf{z}_a and the retrieved state \mathbf{z} . The retrieval is constrained with the data noise and covariance matrices corresponding to the a priori profiles. The constraint matrices are altitude dependent Tikhonov constraints (Kulawik et al., 2006). In this technique, the constraint is optimised for a specified a priori covariance, for which MOZART-3 was used (Brasseur et al, 1998), although the water covariances were scaled up to a 40% variability in the troposphere. The ozone constraint matrices are binned into five latitude bands and the water vapour constraint matrix is the same for all locations on the globe. The constraint matrices can be inverted to yield the a priori error covariance \mathbf{S}_a .

The ozone a priori profile and first guess for the IASI retrievals are the same as for TES. They are generated by merging the climatological monthly mean tropospheric and lower stratospheric ozone field from a 1997-2004 simulation from the MOZART-4 CTM (Emmons et al., 2010) with the climatological monthly mean stratospheric and mesospheric ozone field from a 2005-2010 simulation from the Whole Atmosphere Chemistry-Climate Model (WACCM) model (Kinnison et al., 2007). The a priori profiles are binned by months and by region in 10° latitude and 60° longitude steps. The water vapour a priori profile is taken from the EUMETSAT operational L2. Atmospheric temperature profile and skin temperature are fixed to the IASI EUMETSAT operational L2 values. Other parameters held constant in the retrieval include the CO_2 profile taken from MOZART climatologies, the surface emissivity over land from the Zhou et al. (2011) climatology and the emissivity over water is from Wu and Smith (1997). The IASI scenes are assumed to be cloud-free and were selected with a cloud fraction of less than 13% according to the EUMETSAT operational L2 data. The absorption parameters used in the retrieval are from the TES_v1.4 line parameter database (<http://rtweb.aer.com>) and are pre-calculated. Noise equivalent spectral radiance (NESR) has been estimated at 20 nW / ($\text{cm}^2 \text{ sr cm}^{-1}$) from a set of representative spectra measured in orbit (Clerbaux et al., 2009). The forward model calculates on 67 fixed pressure levels. The retrieval for ozone is performed on 26 levels and for water vapour on 18 levels. The surface pressure is taken from the operational L2 data and the retrieval pressure levels are cropped if necessary at the bottom to reflect the surface pressure.

ERROR ASSESSMENT

Various factors contribute to the overall uncertainty of a retrieved ozone profile, i.e. the smoothing by the retrieval/instrument due to the per se limited information content of the measurement, the data

noise of the instrument, coupling between simultaneously retrieved parameters, and the uncertainties associated with parameters that are not included in the retrieval state vector. The latter include the temperature profile, trace gas profiles for interfering species, spectroscopic parameters of the atmospheric species, the surface temperature, and the emissivity climatology. Further, possible contamination of an IASI scene with clouds can lead to errors if not considered in the retrieval. Additional sources of uncertainty include the IASI instrument calibration and forward model errors associated with discretisation and interpolation of atmospheric profiles. The propagation of these uncertainties into the uncertainty of the atmospheric parameter of interest is sometimes relatively easy, e.g. for the measurement noise. But uncertainties concerning the atmospheric state are rather difficult to quantify since the true state is unknown, e.g. cloud optical parameters. Also instrument calibration errors are unknown (Boynard et al., 2009) and the performance of the radiative transfer model cannot be independently assessed partially due to the fact that the spectroscopic line parameters are not known with sufficient accuracy (Clough et al., 2006). Mathematically, the error covariance can be described as a sum of four terms:

$$\mathbf{S}_z = \underbrace{(\mathbf{A}_{zz} - \mathbf{I}) \mathbf{S}_a (\mathbf{A}_{zz} - \mathbf{I})^T}_{\text{smoothing}} + \underbrace{\mathbf{G} \mathbf{S}_e \mathbf{G}^T}_{\text{measurement}} + \underbrace{\sum \mathbf{G} \mathbf{K}_b \mathbf{S}_b (\mathbf{G} \mathbf{K}_b)^T}_{\text{systematic}} + \underbrace{\sum \mathbf{A}_{xs} \mathbf{S}_a^{\text{bret}} (\mathbf{A}_{xs})^T}_{\text{cross-state}} \quad (3)$$

The first two terms, the smoothing error covariance and the measurement error covariance were mentioned above. The averaging kernel matrix \mathbf{A}_{zz} can be calculated from the gain Matrix \mathbf{G} :

$$\mathbf{A}_{zz} = \mathbf{G} \mathbf{K} \quad (4)$$

where \mathbf{K} is the Jacobian. The averaging kernel describes the sensitivity of the retrieval to the true state. The Jacobian is an output of the radiative transfer model and represents the sensitivity of the forward model towards changes in the retrieved state:

$$\mathbf{K} = \frac{\partial \mathbf{L}(\mathbf{z})}{\partial \mathbf{z}} \quad (5)$$

The gain matrix describes the sensitivity of the retrieved state towards changes in the measured radiances and can be calculated from:

$$\mathbf{G} = (\mathbf{K}^T \mathbf{S}_e^{-1} \mathbf{K} + \mathbf{S}_a^{-1})^{-1} \mathbf{K}^T \mathbf{S}_e^{-1} \quad (6)$$

The measurement noise covariance matrix \mathbf{S}_e is made up of the NESR. Systematic errors originate from fixed parameters b with \mathbf{K}_b and \mathbf{S}_b their respective Jacobians and error covariance matrices. Here, we only calculate how the temperature error propagates into the ozone profile. The temperature error covariance is derived from ensembles of EUMETSAT L2 temperature profiles for specific cases (see below). The cross-state errors stemming from the simultaneous water vapour retrieval is composed of the cross-state part of the averaging kernels \mathbf{A}_{xs} and the water vapour error covariance $\mathbf{S}_a^{\text{bret}}$. The square-root of the diagonal of (3) yields the uncertainty on the ozone profile.

Examples for theoretically calculated errors are shown in Figure 1. The temperature error covariance matrices for the systematic errors were calculated from the ensemble of operational L2 temperature profiles for each set of adjacent IASI scenes. In general, the overall uncertainty, plotted in brown, is dominated by the smoothing error. There are two key empirical methods helping to quantify the actual errors of the retrieval: a) determining the difference of the retrieved profiles with respect to independent measurements, here ozone sondes, and b) determining the range of the deviation from a mean of an ensemble of quasi-coinciding retrieved profiles, i.e. calculating the so-called sample covariance matrix. The square-root of the diagonal of this covariance also serves as a measure to test whether the theoretical errors, limited to the parameters described above, are representative of the true errors.

Systematic errors: validation of IASI ozone profiles with ozone sondes

In order to evaluate systematic errors in the retrieved ozone profiles, they are compared to coincident measurements by ozone sondes. IASI scenes were selected to be within ± 7 hr and ± 110 km of the soundings following Dufour et al. (2012). The averaging kernel matrix \mathbf{A}_{zz} together with the a priori profile $\mathbf{z}_{a \text{ priori}}$ are applied to the sonde profile $\mathbf{z}_{\text{sonde}}$ prior to calculating the bias (Rodgers and Connor, 2003):

$$\hat{\mathbf{z}} = \mathbf{z}_{a \text{ priori}} + \mathbf{A}_{zz} (\mathbf{z}_{\text{sonde}} - \mathbf{z}_{a \text{ priori}}) \quad (7)$$

This new profile $\hat{\mathbf{z}}$ mimics the IASI measurement and retrieval due to the limited vertical sensitivity inherent to remote-sensing techniques. This study focusses on mid-latitudes in 2008. Figure 2 shows

the bias between the retrieved IASI profiles and the ozone sondes separated by location. A list with the sonde station locations together with the number of IASI scenes and ozone soundings used in this comparison is given in Table 1. The coloured lines represent the bias of the individual IASI scenes and the solid black line is the mean. The dotted black lines indicate the 1σ standard deviation of the averaging. A significant positive bias can be observed for most of the comparisons in the upper troposphere/ lower stratosphere (UTLS) region. This bias in ozone is consistent with previous IASI measurements (Dufour et al., 2012), but was also seen in TES retrievals (e.g. Verstraeten et al., 2013). The platform-independent as well as algorithms-independent nature of this bias points towards inaccurate spectroscopic parameters for ozone in the infrared wavelength region as most likely source.

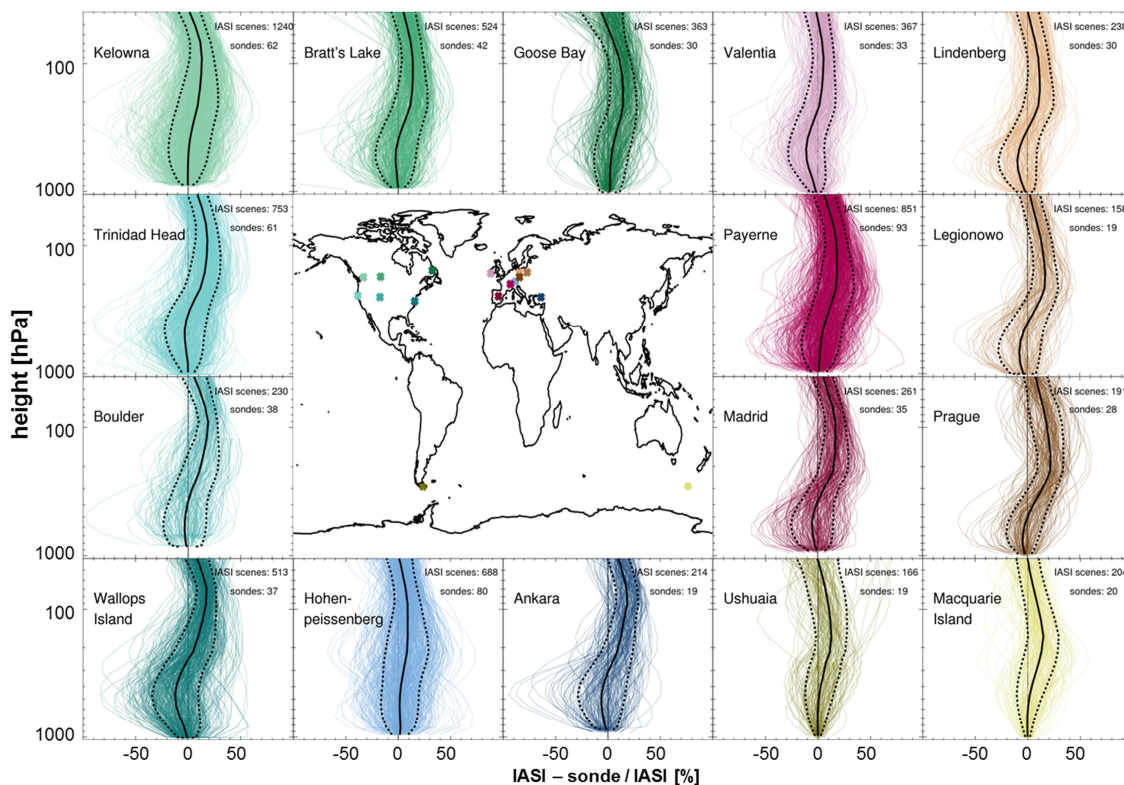


Figure 2: Bias between ozone sondes and IASI ozone profiles for selected mid-latitude location for 2008. Number of IASI scenes and sondes included in this comparison as indicated in the figure and in Table 1. The IASI averaging kernels have been applied to the ozone sonde profiles. Coincidence criteria are ± 7 hr and ± 110 km.

Random errors: comparison of coincident IASI ozone profiles

The difference between adjacent and simultaneous or quasi-simultaneous IASI scenes should not exceed the calculated errors neglecting actual variations in the ozone. This RMS difference of individual profiles with respect to a mean profile of adjacent IASI scenes is an empirical estimate for random errors only. Here we compare the RMS of measured profiles to the combined measurement noise error, the cross-state error from water vapour, and the systematic error from keeping the temperature fixed. We chose one profile with the median IASI viewing angle from the ensemble and assumed that the Jacobians and averaging kernel matrix for this case were representative for all profiles in the ensemble. Results for selected cases are presented in Figure 3. Examples were chosen to be from scenes within a circle with a radius of 110 km around an ozone sonde location (although ozone sonde measurements are not used here). The number of scenes included is stated in the individual plots. The IASI scenes are always from the same orbit. Here, the cloud fraction is less than 6%. In general, the theoretical errors are similar or slightly smaller than the empirical errors. This slight under-estimation could be caused by error sources discussed above, but not included in the calculations here. However, the larger RMS could also reflect some actual variation in the profiles.

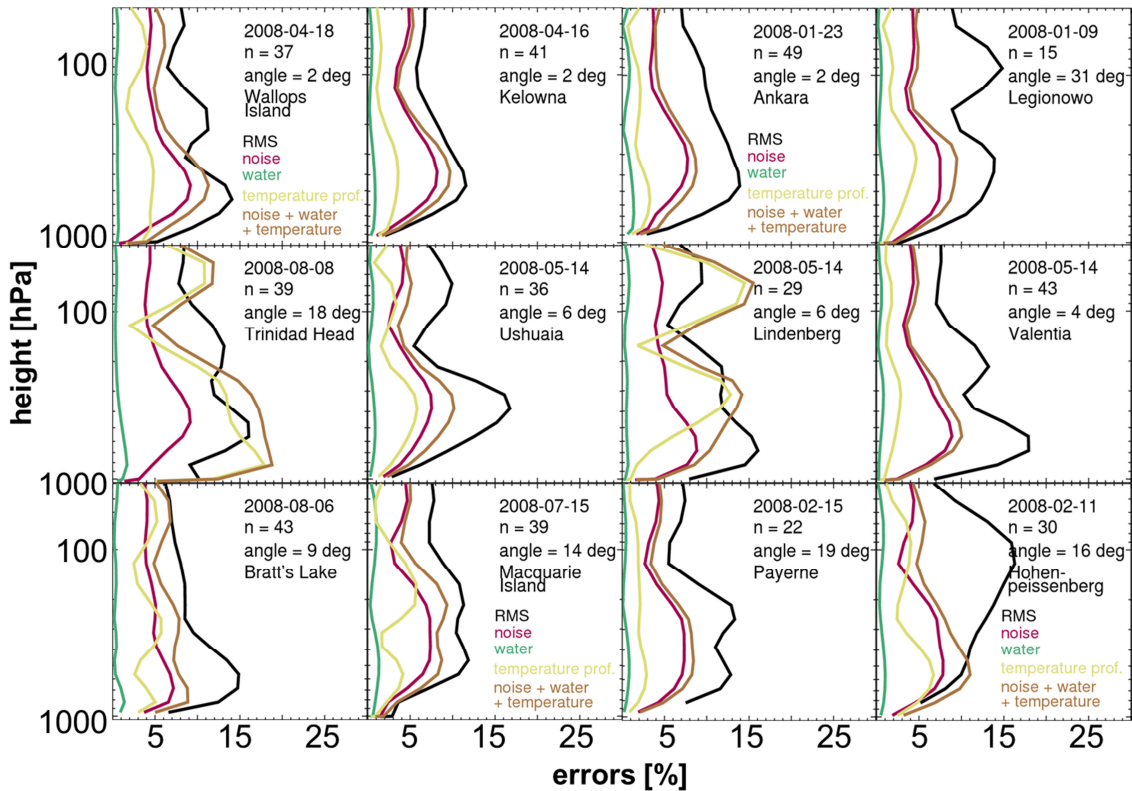


Figure 3: Theoretical and empirical random errors for selected locations as noted in the plots. The number of profiles used is given in the legend of the individual plots as well.

VERTICAL SENSITIVITIES AND DEGREES OF FREEDOM

A meaningful interpretation of a retrieved profile must always include consideration of the vertical sensitivity. Example averaging kernels are shown in Figure 4. The averaging kernels show that IASI is sensitive to ozone in the free troposphere, but has limited or no sensitivity to near-surface ozone. The vertical sensitivity of the retrieval varies according to atmospheric and surface conditions. The trace of the averaging kernel matrix yields the degrees of freedom for signal (DOF) and is summarised in Table 1 for the different locations. DOF depend on the thermal contrast and hence on season. On average, the total DOF are 3.1 ± 0.2 and the tropospheric DOF are 1.0 ± 0.2 with the tropopause height set to 162 hPa, a point of the retrieval grid, which corresponds to about 13 km in the U.S. standard atmosphere.

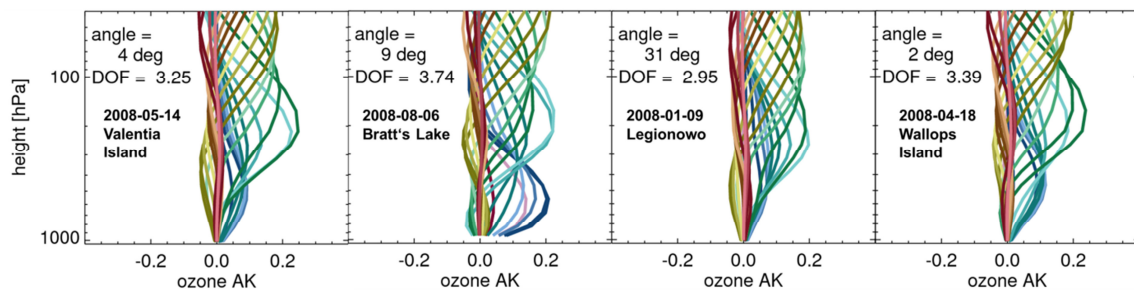


Figure 4: Examples for averaging kernels.

IASI AND TES COMPARISON FOR BRATT'S LAKE

For the ARCTAS field experiment, TES recorded spectra in a stare sequence coinciding with ozone sondes launched among others from Bratt's Lake in 2008 (Boxe et al., 2010). In the stare observation mode, 32 measurements are made for the same location. IASI's coverage naturally yields observation for the same location. Here, the IASI retrievals have been performed in two steps: In a first step the atmospheric temperature profile and surface temperature are retrieved in the CO₂ band with the EUMETSAT operational L2 temperatures as a priori. These retrieved temperatures are then used in the ozone profile retrievals. This 2-step-approach results in a larger number of successfully retrieved ozone profiles and hence better statistics for the comparison. But it is computationally more extensive. Three examples are presented in Figure 5 with at least five satellite scenes per example per instrument as indicated in the legend. The solid lines give the mean of the individual profiles and the dashed lines are the 1 σ standard deviation of the averaging. The TES observations are version 5 of the level 2 data. The raw ozone profile is also overlaid on the figures. The maximum time difference between IASI and TES is 3:26 hr. IASI and TES agree within the uncertainties.

station (elevation above sea level)	latitude	longitude	# of IASI scenes/ sondes	total DOF/ DOF in troposphere
Goose Bay (36 m)	53.3°N	60.4°W	363/ 30	2.84/ 0.90
Legionowo (96 m)	52.4°N	21.0°E	158/ 19	3.31/ 1.16
Lindenberg (112 m)	52.2°N	14.1°E	238/ 30	3.24/ 1.40
Valentia Island (14 m)	51.9°N	10.3°W	367/ 33	3.15 / 1.07
Bratt's Lake (580 m)	50.2°N	104.7°W	524/ 42	3.09/ 1.04
Prague (304 m)	50.0°N	14.4°E	191/ 28	3.03/ 0.95
Kelowna (456 m)	49.9°N	119.4°W	1240/ 62	3.10/ 1.00
Hohenpeißenberg (976 m)	47.8°N	11.0°E	688/ 80	3.17/ 1.07
Payerne (491 m)	46.5°N	6.6°E	851/ 93	3.20/ 1.08
Trinidad Head (20 m)	40.8°N	124.2°W	753/ 61	3.27/ 1.03
Madrid (631 m)	40.5°N	3.6°W	261/ 35	3.43/ 1.20
Boulder (1743 m)	40.0°N	105.3°W	230/ 38	3.32/ 1.08
Ankara (891 m)	40.0°N	32.9°E	214/ 19	3.21/ 1.02
Wallops Island (13 m)	37.9°N	75.5°W	513/ 37	3.38/ 1.17
Macquarie Island (6 m)	54.5°S	158.9°E	204/ 20	2.74/ 0.77
Ushuaia (17 m)	54.9°S	68.3°W	166/ 19	2.76/ 0.78

Table 1: Overview of ozone sonde stations the number of IASI scenes used in this study. Also included are the mean degrees of freedom. Here, the tropopause height is defined to be at 162 hPa.

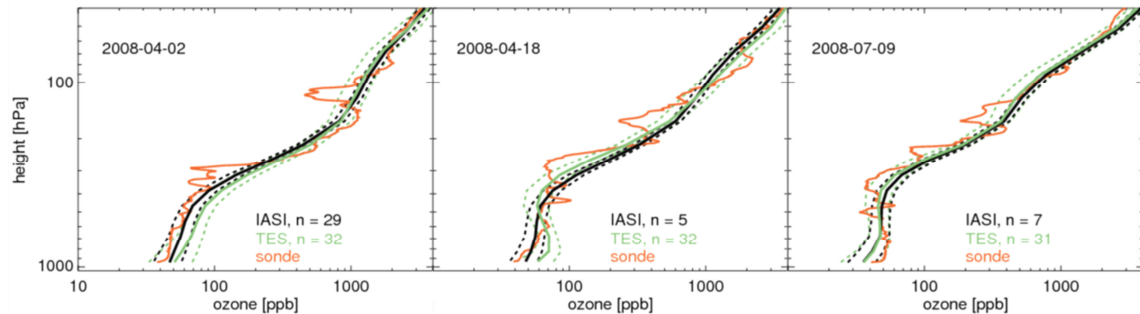


Figure 5: IASI and TES agree within the error bars.

SUMMARY

IASI ozone profiles have been retrieved applying the TES algorithm. The resulting ozone profiles have been validated with ozone sondes. A positive bias in the IASI ozone profiles compared to ozone sondes in the UTLS is found. This is consistent with previous results for IASI (e.g. Dufour et al., 2012) but also for TES (e.g. Verstraeten et al., 2013). The most likely explanation for this bias are incorrect spectroscopic parameters. Empirical and theoretical errors have been retrieved for selected case studies. These two mostly agree and are less than 20 % in the troposphere. On average, the degrees of freedom for signal for the retrieved ozone profiles are 3.1 ± 0.2 for the total atmosphere and 1.0 ± 0.2 for the troposphere. IASI and TES ozone profiles have been compared in three case studies and IASI and TES agree within error bars.

ACKNOWLEDGEMENTS

We acknowledge the NOAA/CLASS data center for the IASI L1C spectra and EUMETSAT for the L2 data. IASI is a joint mission of EUMETSAT and the Centre National d'Etudes Spatiales (CNES, France). The ozone sonde data was provided by the Global Monitoring Division of NOAA (www.esrl.noaa.gmd) and by the World Ozone and Ultraviolet Data Centre (www.woudc.org). Part of the research was carried out at the Jet Propulsion Laboratory, California Institute of Technology, under a contract with the National Aeronautics and Space Administration. We acknowledge NASA support under the grant NNX11AE19G. We thank Cathy Clerbaux (LATMOS, IPSL, France) and Gaëlle Dufour (LISA, France) for discussions.

REFERENCES

- Bowman, K. W., Rodgers, C. D., Kulawik, S. S., Worden, J., Sarkissian, E., Osterman, G., Steck, T., Lou, M., Eldering, A., Shephard, M., Worden, H., Lampel, M., Clough, S., Brown, P., Rinsland, C., Gunson, M., and Beer, R. (2006): Tropospheric emission spectrometer: retrieval method and error analysis, *IEEE Transactions on Geoscience and Remote Sensing*, vol. **44**, no. 5, pp 1297-1307, doi: 10.1109/TGRS.2006.871234.
- Boxe, C. S., Worden, J. R., Bowman, K. W., Kulawik, S. S., Neu, J. L., Ford, W. C., Osterman, G. B., Herman, R. L., Eldering, A., Tarasick, D. W., Thompson, A. M., Doughty, D. C., Hoffmann, M. R., and Oltmans, S. J. (2010): Validation of northern latitude Tropospheric Emission Spectrometer stare ozone profiles with ARC-IONS sondes during ARCTAS: sensitivity, bias and error analysis, *Atmos. Chem. Phys.*, **10**, pp 9901-9914, doi:10.5194/acp-10-9901-2010.
- Boynard, A., Clerbaux, C., Coheur, P.-F., Hurtmans, D., Turquety, S., George, M., Hadji-Lazaro, J., Keim, C., and Meyer-Arnek, J. (2009): Measurements of total and tropospheric ozone from IASI: comparison with correlative satellite, ground-based and ozonesonde observations, *Atmos. Chem. Phys.*, **9**, pp 6255-6271, doi:10.5194/acp-9-6255-2009.
- Brasseur, G. P., Hauglustaine, D. A., Walters, S., Rasch, P. J., Muller, J. F., Granier, C., and Tie, X. X., (1998): MOZART, a global chemical transport model for ozone and related chemical tracers 1. Model description, *J. Geophys. Res. - Atmos.*, vol. **103**, pp 1324-1333.
- Clerbaux, C., Boynard, A., Clarisse, L., George, M., Hadji-Lazaro, J., Herbin, H., Hurtmans, D., Pommier, M., Razavi, A., Turquety, S., Wespes, C., and Coheur, P.-F. (2009): Monitoring of atmospheric composition using the thermal infrared IASI/MetOp sounder, *Atmos. Chem. Phys.*, **9**, pp 6041-6054, doi:10.5194/acp-9-6041-2009.
- Clough, S. A., Shephard, M. W., Worden, J., Brown, P. D., Worden, H. M., Luo, M., Rodgers, C. D., Rinsland, C. P., Goldman, A., Brown, L., Kulawik, S. S., Eldering, A., Lampel, M., Osterman, G., Beer, R., Bowman, K., Cady-Pereira, K. E., and Mlawer, E. J. (2006): Forward model and Jacobians for Tropospheric Emission Spectrometer retrievals, *IEEE Transactions on Geoscience and Remote Sensing*, vol. **44**, no. 5, pp 1308-1323, doi: 10.1109/TGRS.2005.860986.
- Dufour, G., Eremenko, M., Griesfeller, A., Barret, B., LeFlochmoën, E., Clerbaux, C., Hadji-Lazaro, J., Coheur, P.-F., and Hurtmans, D. (2012): Validation of three different scientific ozone products retrieved from IASI spectra using ozonesondes, *Atmos. Meas. Tech.*, **5**, pp 611-630, doi:10.5194/amt-5-611-2012.
- Emmons, L. K., Walters, S., Hess, P. G., Lamarque, J.-F., Pfister, G. G., Fillmore, D., Granier, C., Guenther, A., Kinnison, D., Laepple, T., Orlando, J., Tie, X., Tyndall, G., Wiedinmyer, C., Baughcum, S. L., and Kloster, S. (2010): Description and evaluation of the Model for Ozone and Related chemical Tracers, version 4 (MOZART-4), *Geosci. Model Dev.*, **3**, pp 43-67, doi:10.5194/gmd-3-43-2010.

Kinnison, D. E., Brasseur, G. P., Walters, S., Garcia, R. R., Marsh, D. A., Sassi, F., Boville, B. A., Harvey, L., Randall, C., Emmons, L., Lamarque, J.-F., Hess, P., Orlando, J., Tyndall, G., Tie, X. X., Randel, W., Pan, L., Gettelman, A., Granier, C., Diehl, T., Niemeier, U., and Simmons, A. J. (2007): Sensitivity of Chemical Tracers to Meteorological Parameters in the MOZART-3 Chemical Transport Model., *J. Geophys. Res.*, **112**, D20302, doi:10.1029/2006JD007879.

Kulawik, S. S., Osterman, G., Jones, D. B. A., and Bowman, K. W. (2006): Calculation of altitude-dependent Tikhonov constraints for TES nadir retrievals, *IEEE Transactions on Geoscience and Remote Sensing*, vol. **44**, no. 5, pp 1334-1342, doi: 10.1109/TGRS.2006.871206.

Rodgers, C. D. (2000): *Inverse Methods for Atmospheric Sounding: Theory and Practice*, World Scientific, London.

Rodgers, C. D. and Connor, B. J. (2003): Intercomparison of remote sounding instruments, *J. Geophys. Res.*, **108**, 4116, doi:10.1029/2002JD002299.

Verstraeten, W. W., Boersma, K. F., Zörner, J., Allaart, M. A. F., Bowman, K. W., and Worden, J. R. (2013): Validation of six years of TES tropospheric ozone retrievals with ozonesonde measurements: implications for spatial patterns and temporal stability in the bias, *Atmos. Meas. Tech.*, **6**, pp 1413-1423, doi:10.5194/amt-6-1413-2013.

Wu, X., and Smith, W. L. (1997): Emissivity of rough sea surface for 8–13 μm : modeling and verification, *Appl. Opt.* **36**, pp 2609-2619.

Zhou, D. K., Larar, A. M., Liu, X., Smith, W.L., Strow, L.L., Yang, P., Schlüssel, P., and Calbet, X. (2011): Global Land Surface Emissivity Retrieved From Satellite Ultraspectral IR Measurements," *IEEE Transactions on Geoscience and Remote Sensing*, vol. **49**, no. 4, pp 1277-1290, doi: 10.1109/TGRS.2010.2051036.